# Super-Twisting Control of Double Integrator Systems With Unknown Constant Control Direction

Chau Ton, Siddhartha S. Mehta, and Zhen Kan

***Abstract*—A continuous sliding mode controller is developed for double integrator systems with constant unknown control direction. Additionally, the system is assumed to be subjected to unknown non-vanishing disturbances. The controller yields finite time convergence to hyper sliding surface and guarantees that the origin of the system is exponentially stable. Simulation and experimental results are provided to validate the proposed control algorithm.**

***Index Terms*—Variable-structure/sliding-mode control, robust control, uncertain systems.**

## I. Introduction

UNKNOWN control direction refers to uncertainty in the direction of motion of the system due to uncertainty in the sign of the input gain matrix. Controller design for systems with unknown control direction has been studied for the last three decades. The Nussbaum gain is one of the first adaptive control algorithms developed in [1]. Since its inception, the Nussbaum gain has been widely used in adaptive control to compensate for the input sign uncertainty. However, Nussbaum-based controllers do not guarantee exponential convergence and exhibit peaking phenomenon due to the high-gain feature of these controllers [2], [3], which may pose practical challenges.

Robust control techniques have also been studied for the systems with unknown control direction. Kaloust and Qu [4], presented continuous robust controllers with smooth shifting law to guarantee stability of uniform ultimate boundedness (UUB) with constant and time-varying input sign uncertainties. Sliding mode control (SMC) is a popular robust control technique due to its ability to compensate for parametric uncertainty and external disturbances [5]. Asymptotically stable SMC law was developed in [3] for nonlinear systems with relative degree one and constant unknown control direction. The results were extended in [6] to obtain finite time convergence for systems with relative degree two using a second-order SMC law. Adaptation mechanisms are employed in [6] that vary the sign of the control input gain coefficient to compensate for the unknown control direction. Recently, Oliveira *et al.* [7] and Yan *et al.* [8] developed variable structure model reference controllers, where the constant unknown control direction was identified using monitoring functions. An observer using super-twisting algorithm is designed in [9] to observe the state of a system with unknown control direction. Drakunov *et al.* [10] used a multiple-equilibrium surface to divide the system state space into cells with fixed control to compensate for unknown control direction. For the systems with unknown control direction, the existing continuous robust controllers yield UUB stability and while improved stability guarantees can be obtained using discontinuous SMC, it may result in chattering and large bandwidth actuation.

One of the main aspects of SMC is the design of the sliding surface to which the motion of the system is restricted. To ensure that sliding mode occurs, i.e., the state of the system reaches the sliding manifold, infinite switching is usually required. From a practical perspective, high frequency switching could introduce unwanted oscillations, known as the chattering, that could lead to unintended effects [11]. Various solutions exist in the literature to alleviate the problem of unintended oscillations and chattering in SMC, such as by using a continuous control input within a boundary layer around the sliding surface [12], observers [13], multi-phase converters and appropriate phase shift [14], low-pass filter [15], and gain adaptation [16]. Higher order sliding mode (HOSM) control has also been widely used to mitigate the chattering phenomenon [16], [17]. Generally, HOSM requires that the derivatives of the sliding variables to be known, which may not be desirable in practice. One of the solutions is to use the second order SMC with continuous control structure, also known as super-twisting algorithm (STA). STA facilitates design of a continuous control input without the need for the derivatives of the sliding variables. These benefits motivated variations in the STA algorithm, such as variable gain STA [18], Lyapunov

Manuscript received March 6, 2017; revised May 17, 2017; accepted June 7, 2017. Date of publication June 22, 2017; date of current version July 7, 2017. This work was supported by the AFRL Mathematical Modeling and Optimization Institute Under Grant #FA8651-08-D-0108/042-043-049. Recommended by Senior Editor C. Prieur. *(Corresponding author: Chau Ton.)*

C. Ton is with Air Force Research Laboratory, Kirtland Air Force Base, Albuquerque, NM 87117 USA.

S. S. Mehta is with the University of Florida, Shalimar, FL 32547 USA.

Z. Kan is with the University of Iowa, Iowa City, IA 52246 USA.

Digital Object Identifier 10.1109/LCSYS.2017.2718970

functions for non-homogeneous STA [19], and continuous terminal sliding mode control [20], [21]. Recent results in SMC that alleviate the chattering problem and over estimation of the control gain can be found in [22]–[25].

Motivated by the developments in STA, the goal is to develop a *continuous* robust controller for systems with unknown control direction. Unlike Nussbaum-based adaptive controllers, the system is assumed to be subjected to non-vanishing external disturbances. Specifically, the contribution of this letter is a *continuous* super-twisting sliding mode controller for double integrator systems with constant unknown control direction and non-vanishing disturbances. The presented controller guarantees convergence to hyper sliding surface in finite time, thus identifying the unknown control direction. As opposed to the Nussbaum gain approach [26], the controller guarantees exponential stability of the system origin. The presented controller does not employ logic tests [3], [6] or monitoring functions [7] to determine the hard uncertainty in the control input. Also, in contrast to most SMC-based approaches [7], [8], [10] to systems with input sign uncertainty, the presented control solution is continuous in time. The robustness of the developed controller is verified through numerical simulations and an indoor experiment using a wheeled mobile robot.

This letter is organized in following sections. Section II states the problem formulation and assumptions. Section III defines the sliding surface and open-loop system. Section IV presents the robust control structure and provides stability analysis. Section V contains simulation results, and Section VI presents experimental results. Section VII summarizes the contributions of this letter.

## II. Problem Formulation

Consider an uncertain system with double integrator dynamics subjected to non-vanishing disturbance as

$$\begin{aligned}\dot{x}_1 &= x_2\\ \dot{x}_2 &= f(t) + b(t)u\end{aligned}\tag{1}$$

where $x = [x_1\ x_2]^T \in \mathbb{R}^2$ is the state of the system, $b(t) \in \mathbb{R}$ denotes the uncertain input gain with constant unknown control direction, $f(t) \in \mathbb{R}$ represents the unknown disturbance, and $u(t) \in \mathbb{R}$ is the control input.

*Assumption 1:* The non-vanishing disturbance $f(t)$ and its time-derivative $\dot{f}(t) \in \mathbb{R}$ can be upper bounded by known constants $\bar{f}, \bar{\dot{f}} \in \mathbb{R}^+$ as

$$|f(t)| \le \bar{f}, \quad |\dot{f}(t)| \le \bar{\dot{f}}.$$

*Assumption 2:* The continuous function $b(t)$ in (1) can be written as $b(t) = |b(t)|sign(b(t))$, which satisfies the following properties:

- $|b(t)|$ is lower bounded by a known constant $b_1 \in \mathbb{R}^+$ as $b_1 \le |b(t)|$ such that $b(t) \ne 0 \forall t$.
- The sign of $b(t)$ is constant but unknown, i.e., $sign(b(t)) \in \{1, -1\}$.
- The time-derivative of $b(t)$ is upper bounded by a known constant $\bar{\dot{b}} \in \mathbb{R}^+$ as $|\dot{b}(t)| \le \bar{\dot{b}}$.

*Assumption 3:* The system in (1) is controllable.

The objective is to design a continuous robust control input $u(t)$ that guarantees exponential stability of the system in (1) in the presence of the input sign uncertainty and non-vanishing disturbances.

## III. Sliding Surface Design

Based on the SMC theory, to ensure that (1) converges to the origin, the sliding surface $s(t)$ can be designed as

$$s = \alpha x_1 + x_2 \tag{2}$$

where $\alpha \in \mathbb{R}^+$ is a constant. When the sliding surface $s(t) = 0$, $x_1 = c_0 e^{-\alpha t}$, where $c_0 \in \mathbb{R}$ is a constant, and $x_1(t)$ decays exponentially. To compensate for the sign uncertainty in $b(t)$, the hypersurface $\tilde{s}(t)$ can be designed as

$$\tilde{s} = s + \lambda \int_0^t s(\tau)d\tau \tag{3}$$

where $\lambda \in \mathbb{R}^+$ is a constant.

Taking time derivative of (2) and (3) along the trajectories of (1), the time rate of change of the sliding surface $s(t)$ and the hypersurface sliding surface $\tilde{s}(t)$ can be obtained as

$$\dot{s} = \dot{x}_2 + \alpha x_2 \tag{4}$$

$$\dot{\tilde{s}} = \dot{s} + \lambda s. \tag{5}$$

Substituting (1) and (4) into (5), the open-loop system can be obtained as

$$\dot{\tilde{s}} = b(t)u + \alpha x_2 + f(t) + \lambda s(x). \tag{6}$$

The hypersurface $\tilde{s}(t)$ is used in the subsequent analysis to compensate for the unknown control direction. It will be shown that $\tilde{s}(t)$ approaches a constant in finite time, hence $s(t)$ decays exponentially, and thus the state $x(t)$ exponentially reaches the origin.

## IV. Controller Development

The control input $u(t)$ in (1) is designed below. To facilitate subsequent analysis, $u(t)$ is segregated into two terms as

$$u = k_1 \lceil \Psi \rfloor^{1/2} + \int_0^t u_2(\tau)\, d\tau \tag{7}$$

$$u_2 = (k_2 + \lambda_2|x_2| + \lambda_b|u_3|)sgn(\Psi) - (\lambda + \alpha)u \tag{8}$$

where $k_1, k_2 \in \mathbb{R}^+$ are constants to be defined later, $\lambda_2, \lambda_b \in \mathbb{R}^+$ are known constants, $\lceil \Psi \rfloor^{1/2} = |\Psi|^{1/2} sign(\Psi)$, $u_3 = \int_0^t u_2(\tau)\, d\tau$, and $\Psi(t)$ is a sinusoidal function of $\tilde{s}(t)$ defined as

$$\Psi(t) \triangleq \sin \frac{\pi \tilde{s}}{\varepsilon}$$

where $\varepsilon \in \mathbb{R}^+$ determines the spacing between the equilibrium surfaces.

Using the same super-twisting algorithm as in [18] to represent the sliding surface $s(t)$ as a second order system, the hypersurface $\tilde{s}(t)$ can also be written in the same manner. Substituting (7) into the open-loop system in (6), the closed-loop system can be obtained as

$$\begin{aligned}\dot{\tilde{s}} &= b(t)k_1 \lceil \Psi \rfloor^{1/2} + z\\ \dot{z} &= b(t)(u_2 + (\alpha + \lambda)u) + (\alpha + \lambda)f(t) + \lambda\alpha x_2\\ &\quad + \dot{f}(t) + \dot{b}(t)u_3.\end{aligned}\tag{9}$$

Substituting (8) into the second expression in (9) yields

$$\dot{z} = b(t)(k_2 + \lambda_2|x_2| + |u_3|\lambda_b)sgn(\Psi) + \lambda_1 x_2 + f_1(t) + \dot{b}(t)u_3. \quad (10)$$

where $\lambda_1, \lambda_2 \in \mathbb{R}^+$ such that $\lambda_1 = \lambda\alpha$ and $\frac{\lambda_1}{b_1} \leq \lambda_2$, $\bar{\dot{b}} \leq \lambda_b < (\lambda + \alpha)$ and $f_1(t) = (\alpha + \lambda)f(t) + \dot{f}(t) \leq \delta \in \mathbb{R}^+$. The constants $b_1$ and $\bar{\dot{b}}$ in the above expressions are introduced in Assumption 2, and $k_2$ is designed to satisfy $k_2 \geq \frac{\delta}{b_1}$.

To facilitate subsequent analysis, the term $\dot{z}(t)$ can be succinctly written as

$$\dot{z} = b(t)\rho sgn(\Psi) + f_1(t)$$

where the positive definite function $\rho(t) \in \mathbb{R}$ is expressed as

$$\rho = k_2 + |x_2|\left(\lambda_2 + \lambda_1\frac{sgn(x_2)}{bsgn(\Psi)}\right) + |u_3|\left(\lambda_b + \dot{b}\frac{sgn(u_3)}{bsgn(\Psi)}\right). \quad (11)$$

Let the vector $\zeta(t) \in \mathbb{R}^2$ be defined as

$$\zeta(t) = \begin{bmatrix}\zeta_1\\ \zeta_2\end{bmatrix} \triangleq \begin{bmatrix}\lceil\Psi\rfloor^{1/2}\\ z\end{bmatrix}. \quad (12)$$

Taking time derivative of $\zeta(t)$ along the trajectory in (5), $\dot{\zeta}(t)$ can be obtained as

$$\dot{\zeta} = \frac{1}{|\Psi|^{1/2}}(A\zeta + Bf_2) \quad (13)$$

where the time- and state-varying matrix $A(x,t)$ and the constant vector $B$ can be obtained as

$$A = \begin{bmatrix}\frac{\pi\Omega bk_1}{2\varepsilon} & \Omega\frac{\pi}{2\varepsilon}\\ b\rho & 0\end{bmatrix}, \quad B = \begin{bmatrix}0\\ 1\end{bmatrix}, \quad (14)$$

and $f_2 = |\Psi|^{1/2}f_1(t)$. In (14), $\Omega = \cos\frac{\pi\tilde{s}}{\varepsilon}$.

*Theorem 1:* For the system in (1), where the sign of the input gain $b(t)$ is unknown, provided that $k_1$ and $k_2$ are designed to satisfy inequalities

$$\frac{4(\beta+\gamma^2)}{|b_-\gamma|} > k_1 > max(\mu_1, \mu_2) \quad (15)$$

$$\frac{2\pi|\gamma\Omega|}{2+|\gamma|} > \varepsilon \quad (16)$$

$$(\beta+\gamma^2) > \frac{\varepsilon(|b^+|\rho + |\gamma|)}{2\pi} \quad (17)$$

$$k_2 \geq \frac{\delta}{b_1} \quad (18)$$

where

$$\mu_1 = \frac{\varepsilon^2}{(\beta+\gamma^2)\pi^2\Omega^2}\left(\frac{|\mu_3|}{|b\gamma|} + \frac{|b|\rho^2}{|\gamma|} + \frac{|\gamma|}{|b|} + 2\rho\right) + \frac{1}{4|b\gamma|} + \frac{(|b|\rho + |\gamma|)\varepsilon}{\pi|b\gamma|\Omega^2} \quad (19)$$

$$\mu_2 = \frac{\varepsilon}{(\beta+\gamma^2)\pi|b\Omega|}\mu_3 \quad (20)$$

$$\mu_3 = |b|\Omega\gamma\frac{\pi}{|b|\varepsilon} + 2|\gamma b|\rho + \gamma^2 + f_3^2 + \gamma + 1 \quad (21)$$

and the control input $u(t)$ in (7) ensures that the surface $\tilde{s}(t)$ is reached in finite time, and $(s, x)$ is exponentially stable.

*Proof:* Consider a Lyapunov candidate function $V(t) \in \mathbb{R}^+$ as

$$V = \zeta^T P\zeta \quad (22)$$

where $P \in \mathbb{R}^{2\times 2}$ is a positive definite symmetric matrix given by

$$P = \begin{bmatrix}\beta+\gamma^2 & \gamma\\ \gamma & 1\end{bmatrix} \quad (23)$$

where $\gamma = -k_\gamma sgn(\Omega)$ and $\beta, k_\gamma \in \mathbb{R}^+$ are constants. Taking time derivative of (22) along the trajectories of (1) and substituting (13), the Lyapunov derivative can be obtained as

$$\dot{V} = \frac{1}{|\Psi|^{1/2}}\left(\zeta^T\left(A^TP + PA\right)\zeta + 2f_2B^TP\zeta\right) + \zeta^T\dot{P}\zeta \quad (24)$$

where the fact that $B^TP\zeta = \zeta^TPB$ is used.

*Remark 1:* Consider a set where $\tilde{s} = \{\epsilon/2, 3\epsilon/2, 5\epsilon/2, \ldots\}$. In this set $\Omega = 0$, hence $\dot{\gamma} = -k_\gamma\delta$, where $\delta$ is the Dirac delta function. Although $\dot{\gamma}$ is singular, $V(t)$ does not immediately go to infinity due to the property $\int_{\gamma=-\infty}^{\gamma=\infty}\delta(\gamma)d\gamma = 1$. Fox example, consider the case when the states are on an unattractive manifold, i.e., $\tilde{s} = \varkappa + \varepsilon$, where $\varkappa = 0, \pm\varepsilon, \pm 2\varepsilon, \pm 3\varepsilon, \ldots$. This implies in (9) that the hypersurface $\tilde{s}(t)$ increases to another constant $\tilde{s} = \varkappa + 2\varepsilon$ or decreases to $\tilde{s} = \varkappa$, where both surfaces are attractive. This also implies that $\Omega$ continuously increases from -1 to 1, or decreases from 1 to -1, while crossing the boundary $\Omega = 0$. Although $\dot{\gamma} = -k_\gamma\delta$ when $\Omega = 0$, the control input $u(t)$ is continuous and the actual system in (1) does not jump. Hence, the discontinuity at $\Omega = 0$ can be regarded as a jump from an unattractive set towards an attractive set. It will be shown that the system is stable as $\Omega \to \pm 1$, and $\Omega$ only crosses the boundary $\Omega = 0$ when it goes from an unattractive to attractive region. Also note that $\Omega = 0$ does not correspond to the equilibrium point. Therefore, the following analysis ignores the case when $\Omega = 0$ and hence $\dot{P} = 0$ is used in (24).

Let $f_3 \in \mathbb{R}^+$ be a known constant where $(\alpha+\lambda)\bar{f} + \bar{\dot{f}} \leq f_3$, where $\bar{f}$ and $\bar{\dot{f}}$ are defined in Assumption 1, then the Lyapunov derivative can be upper bounded as

$$\dot{V} \leq \frac{1}{|\Psi|^{1/2}}\left(\zeta^T\xi\zeta + 2f_2B^TP\zeta + f_3^2|\Psi| - f_2^2\right) \quad (25)$$

where $\xi = A^TP + PA$. After completing the squares and using $f_3^2|\Psi| = f_3^2\zeta^TC^TC\zeta$ for $C = [1 \quad 0]$, the inequality in (25) can be written as

$$\dot{V} \leq \frac{1}{|\Psi|^{1/2}}\zeta^TQ\zeta \quad (26)$$

where $Q(t) \in \mathbb{R}^{2\times 2}$ is as follows:

$$Q = \begin{bmatrix}\upsilon & \chi\\ \chi & \frac{\gamma\pi}{\varepsilon}\Omega + 1\end{bmatrix}. \quad (27)$$

The scalar functions $\chi(t), \upsilon(t) \in \mathbb{R}$ in (27) can be obtained as

$$\chi = \frac{\pi}{2\varepsilon}\Omega\left((\beta+\gamma^2) + b\gamma k_1\right) + \gamma + b\rho \quad (28)$$

$$\upsilon = b\Big((\beta+\gamma^2)\frac{\pi}{\varepsilon}k_1\Omega + 2\gamma\rho\Big) + \gamma^2 + f_3^2. \tag{29}$$

The objective is to ensure $Q(t)$ to be negative definite. Let $Q_1(t) = -Q(t)$ and the inequality

$$Q_2 = Q_1 - \frac{|\gamma|}{2}I > 0 \tag{30}$$

is satisfied, where $I \in \mathbb{R}^{2\times 2}$ is the identity matrix. Then, $Q_2(t)$ can be expressed as

$$Q_2 = -\begin{bmatrix} \upsilon + |\gamma|/2 & \chi \\ \chi & \sigma \end{bmatrix} \tag{31}$$

where $\sigma(t) = \frac{\gamma\pi}{\varepsilon}\Omega + 1 + \frac{|\gamma|}{2}$.

For unknown $sign(b(t))$, when the sliding surface $\tilde{s}(t) = \Xi$ is attractive, where $\Xi$ is a constant, the sign of $\Omega$ always converges to the opposite of the sign of $b(t)$, i.e., $sgn(\Omega) = -sgn(b(t))$. This implies that $sgn(b\Omega) = -1$ when $sgn(\Psi)$ is attractive, otherwise $sgn(b\Omega) = 1$. However, when $sgn(\Psi)$ is not attractive, the state $\tilde{s}(t)$ leaves the current manifold and enters the region where $sgn(\Psi)$ is attractive.

Recall that the eigenvalues are related to the determinant and trace of the matrix as

$$det(Q_2) = \eta_1\eta_2, \quad trace(Q_2) = \eta_1 + \eta_2 \tag{32}$$

where $\eta_1$ and $\eta_2$ are the eigenvalues of $Q_2(t)$. When $det(Q_2) > 0$ and $trace(Q_2) > 0$, this implies that the eigenvalues $\eta_1, \eta_2 > 0$ and the matrix $Q_2(t)$ is positive definite. To ensure that $Q_2(t)$ has positive eigenvalues, using the expressions in (32) and the attractive properties of $sgn(\Psi)$, the inequalities in (15)-(18) have to be satisfied.

In the set $\mathcal{F} = \{(\Omega, \rho, b)|0 < |\Omega|, \rho < \bar{\rho}, b_1 \leq |b|\}$, where $\bar{\rho} \in \mathbb{R}^+$ is a constant and $b_1$ is defined in Assumption 2, there exist a positive constant $\beta$, a function $\gamma(t)$, and a positive constant $k_1$ that satisfy inequalities (15)-(17). It can be seen that by increasing the constant $\beta$, inequalities (15) and (17) can be easily satisfied. Therefore, using (30) and the fact that $Q_1(t) = -Q(t)$, the Lyapunov derivative can be upper bounded as

$$\dot{V}_1 \leq -\frac{|\gamma|}{2}\frac{\|\zeta\|^2}{|\Psi|^{1/2}} \tag{33}$$

where $\|\cdot\|$ denotes the Euclidean norm. From (12), it is clear that $\|\zeta\| > |\Psi|^{1/2}$. Using this fact and the definition of $\gamma$ in (23), the inequality in (33) can be expressed as

$$\dot{V}_1 \leq -\frac{k_\gamma}{2}\|\zeta\|. \tag{34}$$

The Lyapunov function $V(t)$ in (22) can be upper and lower bounded as

$$\Lambda_{\min}(P)\|\zeta\|^2 \leq V \leq \Lambda_{\max}(P)\|\zeta\|^2$$

where $\Lambda_{\min}(P)$ and $\Lambda_{\max}(P)$ are the minimum and maximum eigenvalues of $P$, respectively. Therefore, the Lyapunov derivative in (34) can be further upper bounded as

$$\dot{V}_1 \leq -\frac{k_\gamma}{2\Lambda_{\max}(P)}V_1^{1/2}. \tag{35}$$

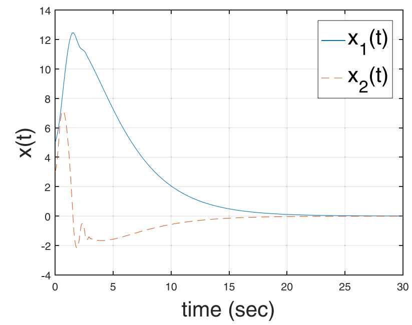


Fig. 1. Position $x_1(t)$ and velocity $x_2(t)$ versus time showing exponential convergence of the states to the origin.

The inequality in (35) implies that $V(t)$ goes to zero in finite time [18]. This implies that $\tilde{s}(t)$ goes to a constant in finite time. Therefore, (5) yields the following equality [10]:

$$\dot{s} = -\lambda s. \tag{36}$$

From (36), it is clear that $s(t)$ exponentially decays to zero. Given the fact that $s(t) \to 0$, it can easily be shown from (2) and (4) that $x(t) \to 0$ as $t \to \infty$ [10].

Similar to [18], the proposed control structure cannot stay on the set $\mathcal{S} = \{(\Psi, z) \in \mathbb{R}^2|\Psi = 0\}$. Since $V(t)$ is continuously decreasing, by using [27, Proposition 14.1], where $\dot{V}(t)$ does not need to be differentiable, it can be concluded that the equilibrium $(\Psi, z)$ can be reached in finite time from any initial condition. ■

## V. Simulation Results

Simulation for the second order systems in (1) was carried out to validate the robustness of the proposed controller. Various control gains and design parameters used in the control law were selected as

$$k_1 = 1.0 \quad k_2 = 18 \quad \alpha = 0.5 \quad \lambda = 0.3$$
$$\varepsilon = 10 \quad \lambda_2 = 0.35 \quad \lambda_b = 0.034$$

The non-vanishing disturbance $f(t)$ and the unknown input gain $b(t)$ were selected as the following functions of time:

$$f(t) = 5\sin(t), \quad b(t) = 1 + 0.5\cos(t/30).$$

Although the direction of the control input, i.e., $sign(b(t)) = 1$, was specified, it was not used in the controller development. In addition, the magnitude of $b(t)$ was considered to be unknown and only a lower bound on $|b(t)|$ was used to satisfy the gain conditions. The initial conditions were given as

$$x_1(0) = 5, \quad x_2(0) = 3.$$

Figure 1 shows the position $x_1(t)$ and velocity $x_2(t)$, Figure 2 shows the surface $s(t)$ and the hypersurface $\tilde{s}(t)$, and Figure 3 shows the control input $u(t)$ as a function of the time. In Figure 2, it can be seen that $\tilde{s}(t)$ reaches a constant in finite time and consequently $s(t)$ goes to zero exponentially, which implies that $x(t)$ goes to zero exponentially as shown in Figure 1. It can be seen that the control input $u(t)$ in Figure 3 is continuous, and the chattering phenomenon is mitigated.

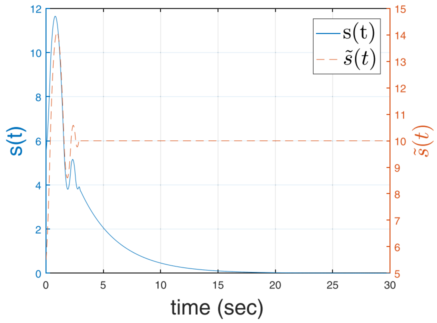


Fig. 2. Surface $s(t)$ and hypersurface $\tilde{s}(t)$ versus time showing finite time convergence of the hypersurface $\tilde{s}(t)$ and exponential convergence of the surface $s(t)$.

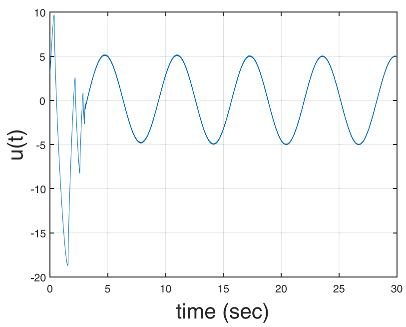


Fig. 3. Control input $u(t)$ versus time.

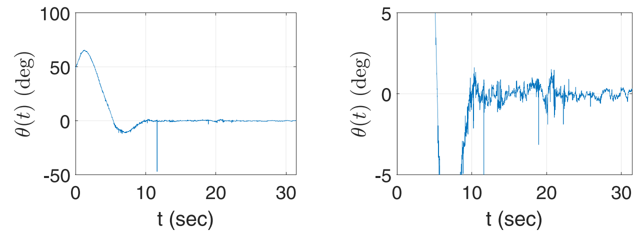


(a) $\theta(t)$ (b) $\theta(t)$ zoomed in

Fig. 4. The angular position of the robot $\theta(t)$ versus time.

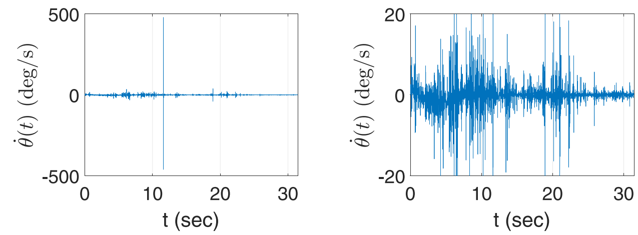


(a) $\dot{\theta}(t)$ (b) $\dot{\theta}(t)$ zoomed in

Fig. 5. The angular velocity of the robot $\dot{\theta}(t)$ versus time.

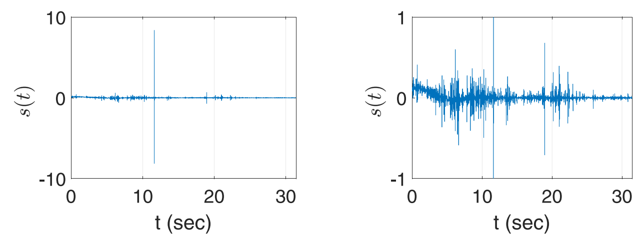


(a) $s(t)$ (b) $s(t)$ zoomed in

Fig. 6. The surface $s(t)$ versus time.

## VI. Experimental Results

To demonstrate the effectiveness of the proposed control structure, an experiment was carried out using iRobot Create. iRobot Create is a differential drive wheeled mobile robot. The dynamics of the robot are given by

$$\begin{bmatrix} \ddot{x} \\ \ddot{y} \\ \ddot{\theta} \end{bmatrix} = \begin{bmatrix} \dot{\upsilon}\cos\theta - \upsilon\dot{\theta}\sin\theta \\ \dot{\upsilon}\sin\theta + \upsilon\dot{\theta}\cos\theta \\ b(t)u + f(t) \end{bmatrix} \tag{37}$$

where $(x, y)$ is the position of the robot in the $xy$-plane, $\upsilon$ is the linear velocity of the robot, $\theta(t)$ is the orientation of the robot measured counter-clockwise with respect to $x$-axis, $u(t)$ is the control input (i.e., angular acceleration), $b(t)$ is the unknown input gain, and $f(t)$ is the unknown disturbance. The control objective was to stabilize the orientation $\theta(t)$ and angular velocity $\dot{\theta}(t)$ to the origin in the presence of sign uncertainty, i.e., $\theta(t), \dot{\theta}(t) \to 0$. In other words, the goal is to regulate the orientation of the robot to 0 or parallel to $+x$-axis, and the position $(x, y)$ can be anywhere in the workspace. As the objective is to regulate the orientation of the robot, the linear velocity $\upsilon(t)$ was held constant at 0.2 $m/s$ throughout the time. The time-varying angle and position of the robot with respect to the inertial frame was measured using an OptiTrack Motion Capture system. The controller was implemented in Robotic Operating System (ROS) and received state feedback from OptiTrack over a wireless network. The robot uses a low-level velocity controller, and therefore the angular acceleration input $u(t)$ was integrated to obtain commanded angular velocity to drive the robot. Note that although the mobile robot is nonholonomic, only the orientation of the robot is controlled where the orientation sub-system is fully actuated. In practice, the disturbance $f(t)$ may not be known *a priori*. However, from the knowledge of the workspace or the environment, a bound on $f(t)$ can be established. In this experiment, the disturbance was due to imperfections in the floor (e.g., bumps) which were sufficiently smooth. Therefore, $f(t)$ and $\dot{f}(t)$ exist and can be considered to be bounded, and the control gain was tuned sufficiently large to compensate for $f(t)$. The results are shown in Figures 4–8.

Various control gains and constant design parameters in (2), (3), (7), and (8) were selected as

$$k_1 = 0.1 \quad k_2 = 0.2 \quad \alpha = 0.1 \quad \lambda = 0.1$$
$$\varepsilon = 0.25 \quad \lambda_2 = 0.11 \quad \lambda_b = 0.01$$

Figures 4–8 show the angle $\theta(t)$, angular velocity $\dot{\theta}(t)$, surface $s(t)$, hypersurface $\tilde{s}(t)$, and control input $u(t)$ as a function of time. The hypersurface $\tilde{s}(t)$ approaches a constant in approximately 7s as shown in Figure 7, which causes $s(t)$, $\theta(t)$, and $\dot{\theta}(t)$ to exponentially decays to zero as shown in Figures 4-6. The large spike in Figures 4-7 and 9 was due to momentary loss of track from the OptiTrack system, however, that did not drastically affect the performance of the controller. The angular velocity $\dot{\theta}(t)$ was noisy due to noisy measurement

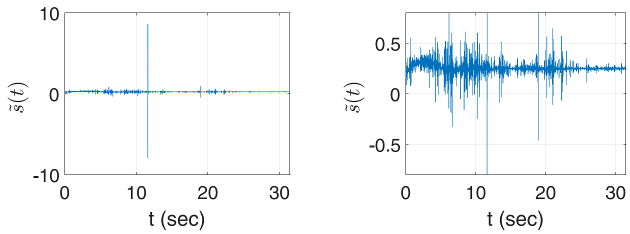


(a) $\tilde{s}(t)$ (b) $\tilde{s}(t)$ zoomed in

Fig. 7. The hypersurface $\tilde{s}(t)$ versus time.

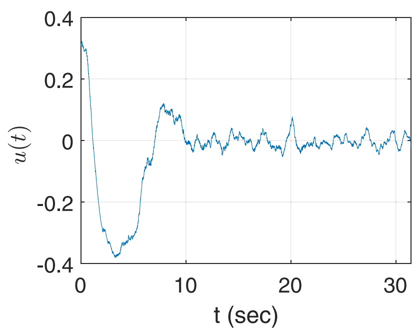


Fig. 8. Control input $u(t)$ versus time.

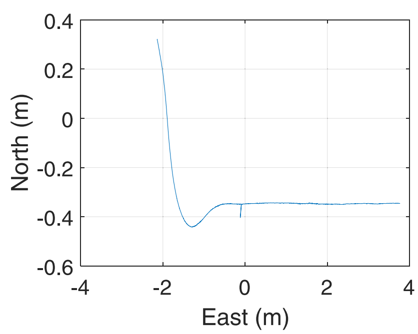


Fig. 9. Robot's trajectory in the workplace shows the robot tracks a straight line as $\theta(t) \to 0$.

from $\theta(t)$. Figure 9 shows the position of the robot in the workspace. It can be seen that the robot travels in a straight line as $\theta(t)$ approaches zero.

## VII. Conclusion

A continuous sliding mode controller is developed for second-order systems with constant unknown control direction. The presented controller guarantees that the unknown sign of the control gain can be identified in a finite time as the designed hypersurface converges to a constant manifold. Further, once the control direction is identified, the controller guarantees that the origin of the system is exponentially stable. Simulation and experimental results demonstrate the effectiveness of the control algorithm.

## References

[1] R. D. Nusssbaum, "Some remarks on a conjecture in parameter adaptive control," *Syst. Control Lett.*, vol. 3, no. 5, pp. 243–246, 1983.

[2] J. C. Willems and G. I. Byrnes, "Global adaptive stabilization in the absence of information on the sign of the high frequency gain," in *Analysis and Optimization of Systems*. Heidelberg, Germany: Springer, 1984, pp. 49–57.

[3] G. Bartolini, A. Ferrara, and L. Giacomini, "A switching controller for systems with hard uncertainties," *IEEE Trans. Circuits Syst. I, Fundam. Theory Appl.*, vol. 50, no. 8, pp. 984–990, Aug. 2003.

[4] J. Kaloust and Z. Qu, "Robust control design for nonlinear uncertain systems with an unknown time-varying control direction," *IEEE Trans. Autom. Control*, vol. 42, no. 3, pp. 393–399, Mar. 1997.

[5] V. Utkin, "Variable structure systems with sliding modes," *IEEE Trans. Autom. Control*, vol. 22, no. 2, pp. 212–222, Apr. 1977.

[6] G. Bartolini, A. Pisano, and E. Usai, "On the second-order sliding mode control of nonlinear systems with uncertain control direction," *Automatica*, vol. 45, no. 12, pp. 2982–2985, 2009.

[7] T. R. Oliveira, A. J. Peixoto, E. V. L. Nunes, and L. Hsu, "Control of uncertain nonlinear systems with arbitrary relative degree and unknown control direction using sliding modes," *Int. J. Adapt. Control Signal Process.*, vol. 21, nos. 8–9, pp. 692–707, 2007.

[8] L. Yan, L. Hsu, R. R. Costa, and F. Lizarralde, "A variable structure model reference robust control without a prior knowledge of high frequency gain sign," *Automatica*, vol. 44, no. 4, pp. 1036–1044, 2008.

[9] E. Guzmán and J. A. Moreno, "Super-twisting observer for second-order systems with time-varying coefficient," *IET Control Theory Appl.*, vol. 9, no. 4, pp. 553–562, Feb. 2015.

[10] S. Drakunov, U. Ozguner, P. Dix, and B. Ashrafi, "ABS control using optimum search via sliding modes," *IEEE Trans. Control Syst. Technol.*, vol. 3, no. 1, pp. 79–85, Mar. 1995.

[11] V. I. Utkin, *Sliding Modes in Control and Optimization*. Berlin, Germany: Springer-Verlag, 1992.

[12] P. Kachroo and M. Tomizuka, "Chattering reduction and error convergence in the sliding-mode control of a class of nonlinear systems," *IEEE Trans. Autom. Control*, vol. 41, no. 7, pp. 1063–1068, Jul. 1996.

[13] G. Bartolini and P. Pydynowski, "An improved, chattering free, VSC scheme for uncertain dynamical systems," *IEEE Trans. Autom. Control*, vol. 41, no. 8, pp. 1220–1226, Aug. 1996.

[14] H. Lee, V. I. Utkin, and A. Malinin, "Chattering reduction using multiphase sliding mode control," *Int. J. Control*, vol. 82, no. 9, pp. 1720–1737, 2009.

[15] M.-L. Tseng and M.-S. Chen, "Chattering reduction of sliding mode control by low-pass filtering the control signal," *Asian J. Control*, vol. 12, no. 3, pp. 392–398, 2010.

[16] V. I. Utkin and A. S. Poznyak, "Adaptive sliding mode control with application to super-twist algorithm: Equivalent control method," *Automatica*, vol. 49, no. 1, pp. 39–47, 2013.

[17] A. Levant, "Principles of 2-sliding mode design," *Automatica*, vol. 43, no. 4, pp. 576–586, 2007.

[18] T. Gonzalez, J. A. Moreno, and L. Fridman, "Variable gain super-twisting sliding mode control," *IEEE Trans. Autom. Control*, vol. 57, no. 8, pp. 2100–2105, Aug. 2012.

[19] J. A. Moreno, "On strict Lyapunov functions for some non-homogeneous super-twisting algorithms," *J. Frankl. Inst.*, vol. 351, no. 4, pp. 1902–1919, 2014.

[20] S. Kamal, J. A. Moreno, A. Chalanga, B. Bandyopadhyay, and L. M. Fridman, "Continuous terminal sliding-mode controller," *Automatica*, vol. 69, pp. 308–314, Jul. 2016.

[21] V. Torres-González, T. Sanchez, L. M. Fridman, and J. A. Moreno, "Design of continuous twisting algorithm," *Automatica*, vol. 80, pp. 119–126, Jun. 2017.

[22] J. A. Moreno, D. Y. Negrete, V. Torres-González, and L. Fridman, "Adaptive continuous twisting algorithm," *Int. J. Control*, vol. 89, no. 9, pp. 1798–1806, 2016.

[23] G. Bartolini, A. Levant, A. Pisano, and E. Usai, "Adaptive second-order sliding mode control with uncertainty compensation," *Int. J. Control*, vol. 89, no. 9, pp. 1747–1758, 2016.

[24] F. Plestan, Y. Shtessel, V. Brégeault, and A. Poznyak, "Sliding mode control with gain adaptation—Application to an electropneumatic actuator," *Control Eng. Pract.*, vol. 21, no. 5, pp. 679–688, 2013.

[25] C. Edwards and Y. Shtessel, "Adaptive continuous higher order sliding mode control," *IFAC Proc. Vol.*, vol. 47, no. 3, pp. 10826–10831, 2014.

[26] W. Chen, X. Li, W. Ren, and C. Wen, "Adaptive consensus of multi-agent systems with unknown identical control directions based on a novel Nussbaum-type function," *IEEE Trans. Autom. Control*, vol. 59, no. 7, pp. 1887–1892, Jul. 2014.

[27] K. Deimling, *Multivalued Differential Equations*, vol. 1. Berlin, Germany: Walter de Gruyter, 1992.